physica status solidi rrl
www.pss-rapid.com

Enhanced AlScN/GaN Heterostructures Grown with a Novel Precursor by Metal–Organic Chemical Vapor Deposition

Isabel Streicher, Stefano Leone, Lutz Kirste, Christian Manz, Patrik Straňák, Mario Prescher, Patrick Waltereit, Michael Mikulla, Rüdiger Quay, and Oliver Ambacher*

Growth of AlScN high-electron-mobility transistor (HEMT) structures by metal–organic chemical vapor deposition (MOCVD) is challenging due to the low vapor pressure of the conventionally used precursor tris-cyclopentadienyl-scandium (Cp_3Sc). It is shown that the electrical and structural characteristics of the AlScN/GaN heterostructure improve significantly by using bis-methylcyclopentadienyl-scandiumchloride ($(MCp)_2ScCl$), which has a higher vapor pressure and allows for an increased molar flow and thus higher growth rate (GR). AlScN/GaN HEMT heterostructures with superior electrical characteristics deposited at different barrier growth temperatures are presented. The sheet resistance R_{sh} of $172\,\Omega\,sq^{-1}$ obtained at 900 °C barrier growth temperature is among the lowest reported so far for AlScN/GaN HEMT structures. The sheet charge carrier density n_s is $3.23 \times 10^{13}\,cm^{-2}$ and the electron mobility μ is $1124\,cm^2\,Vs^{-1}$.

1. Introduction

Energy-efficient high-power and high-frequency devices are needed to reach the full potential of renewable energy sources, especially in energy conversion but also for efficient data transmission. GaN-based high-electron-mobility transistors (HEMTs) with AlGaN barriers provide the required high breakdown voltages and high power density and output power at high frequencies, and are already on the market.[1–3] The device performance can be boosted further with AlScN as barrier material which, thanks to the increased gradient of spontaneous and piezoelectric polarization between AlScN and GaN, provides higher sheet charge carrier densities (n_s) in the 2D electron gas (2DEG) at the barrier/channel-interface and thus a reduced channel resistance.[4–6] $Al_{0.82}Sc_{0.18}N$ is lattice-matched to GaN and thus theoretically infinitely thick barriers are accessible without the generation of stress-related defects and cracks,[7] unlike AlN barriers which are strongly limited by their low critical thickness of <5 nm on GaN.[8] Molecular beam epitaxy (MBE) is used to grow high-quality AlScN on GaN,[9–13] but metal–organic chemical vapor deposition (MOCVD) is the preferred method for industrial-scale production. A major challenge to the MOCVD growth of AlScN is the Sc precursor. Complexes of transition metals like Sc (group 3 or IIIB) have a lower vapor pressure than complexes from metals of group 13- or IIIA-nitrides, like Al and Ga. The growth of Sc-containing nitrides by MOCVD was not successful and Sc was incorporated on doping levels only,[14,15] until we developed a proprietary heating and gas mixing system tailored to the usage of precursors with low vapor pressure such as commercially available Cp_3Sc.[16] We examined the effect of the growth parameters temperature, growth mode, V/III ratio, and pressure on the growth of AlScN with Cp_3Sc.[17] Furthermore, we evaluated GaN and SiN_x cap layers and the diffusion behavior of Al-, Sc-, and Ga-atoms.[18] The first MOCVD-grown AlScN HEMT structures we demonstrated had a drain current of $1720\,mA\,mm^{-1}$ and a transconductance of $530\,mS\,mm^{-1}$.[18] The sheet resistance R_{sh} was $323\,\Omega\,sq^{-1}$, the sheet charge carrier density n_s $2.6 \times 10^{13}\,cm^{-2}$, and the electron mobility μ $729\,cm^2\,Vs^{-1}$. These values are close to but below what can be achieved with MBE.

Due to the low vapor pressure of Cp_3Sc, the molar flow to the reactor remains low and leads to very low GRs ($0.006\,nm\,s^{-1}$). This results in long growth times during which the epilayers are exposed to the high growth temperature. This promotes the diffusion of atoms at the interfaces. Especially Al atoms

I. Streicher, S. Leone, L. Kirste, C. Manz, P. Straňák, M. Prescher, P. Waltereit, M. Mikulla, R. Quay
Business Unit Power Electronics
Fraunhofer Institute for Applied Solid State Physics IAF
Tullastrasse 72, 79108 Freiburg, Germany
E-mail: isabel.streicher@iaf.fraunhofer.de

O. Ambacher
Institute for Sustainable Systems Engineering (INATECH)
University of Freiburg
Emmy-Noether-Strasse 2, 79110 Freiburg, Germany

The ORCID identification number(s) for the author(s) of this article can be found under https://doi.org/10.1002/pssr.202200387.

DOI: 10.1002/pssr.202200387

are known for diffusing easily into GaN when HEMT structures are exposed to a high thermal budget, either during MOCVD growth or annealing of MBE samples.[19,20] Graded AlGaN interlayers form and lead to a broadening of the potential well and the charge carrier distribution in the 2DEG. We showed that the barrier/channel interface can be improved to some extent by inserting a nominal AlN interlayer or reducing the growth temperature.[21]

To date, there is no other report in the literature of MOCVD of AlScN reporting GRs higher than 0.006 nm s^{-1}. An enhancement in GR is necessary to reduce the degradation of the barrier/channel interface by diffusion during high-temperature MOCVD growth. Besides, having high GRs can open the way to the deposition of thick AlScN layers for numerous applications, such as ferroelectric layers for non-volatile memories, which have recently been demonstrated by both reactive sputter deposition[22] and MBE,[23] or RF-filters, and many more.

In this work, we report on an increase in the AlScN GR using the novel precursor bis-methylcyclopentadienyl-scandium chloride ($(MCp)_2ScCl$), which has a more than ten times higher vapor pressure than the standard Sc precursor Cp_3Sc.[24] We show that this boosts the electrical properties of AlScN HEMT structures grown on 4H-SiC (00.1) and Al_2O_3 (00.1) significantly and allows for higher Sc contents at a given growth temperature.

$(MCp)_2ScCl$ has its melting point at 155 °C and boiling point at 160 °C,[24] which is close to the setup temperature of 150 °C we used so far for the growth of AlScN using solid Cp_3Sc as Sc-precursor.[16] To reach the highest possible amount of Sc precursor in the gas phase and to profit from the increased stability in the molar flow that comes with a liquid precursor, we increased the source temperature to 155 °C. We observed that $(MCp)_2ScCl$ is highly sensitive to the stability of the heating of the source and the gas injection system. Any discontinuities or oscillations in the heating can cause condensation and re-evaporation of the material, which leads to spikes in the scandium concentration of the grown layers. As proposed in our patent application,[25,26] we now use an oven for heating the source and a gas injection system heated slightly above the oven temperature. Respecting these technical requirements, AlScN HEMT structures with strongly improved properties are grown.

In the following, we will focus on: 1) morphology, 2) structural quality, 3) compositional characterization, and 4) electrical properties. We will compare the samples grown with the new precursor $(MCp)_2ScCl$ with its maximum GR of 0.015 nm s^{-1} to samples grown with Cp_3Sc grown with its maximum GR of 0.006 nm s^{-1}. Growth conditions and layer thicknesses are the same.

2. Results and Discussion

2.1. Morphology

A smooth morphology is important for device fabrication. The AlScN HEMT structures capped with an amorphous in situ SiN_x cap have a very smooth morphology.[18] The root mean square (RMS) average of $10 \times 10\ \mu m^2$ scans was determined with atomic force microscopy (AFM) in tapping mode. Layers grown with $(MCp)_2ScCl$ as Sc precursor with increased GR and consequently reduced growth time, have a smooth surface at both 900 and 1200 °C with RMS values of 0.31 and 0.58 nm, respectively, as shown in **Figure 1**a,b. In contrast, a barrier layer grown at 1200 °C with the same V/III ratio but Cp_3Sc as Sc precursor, and thus very low GR, cannot be stabilized by ammonia and localized etching occurs. The layer decomposes preferentially in the outcrop area of defects leaving wide hexagonal pits, as shown in Figure 1c. The RMS value is as high as 4.6 nm. Even though the best electrical performances were achieved at low barrier growth temperatures, the ability to grow HEMT structures with smooth morphologies also at high temperatures is important, as these structures are more robust when it comes to high-temperature annealing processes in device manufacturing. In case the annealing temperature exceeds the barrier growth temperature, the high thermal budget can promote diffusion at the interface and degrade it.[19,20]

2.2. Structural Characterization

High-resolution X-Ray diffractometry (HRXRD) Θ/2Θ -scans of the 00.2 reflection range for the AlScN HEMT structures grown at different temperatures with the two precursors are shown in **Figure 2**. Besides the strong and sharp reflections of the 4H-SiC substrate, the GaN buffer layers and the AlN nucleation layer

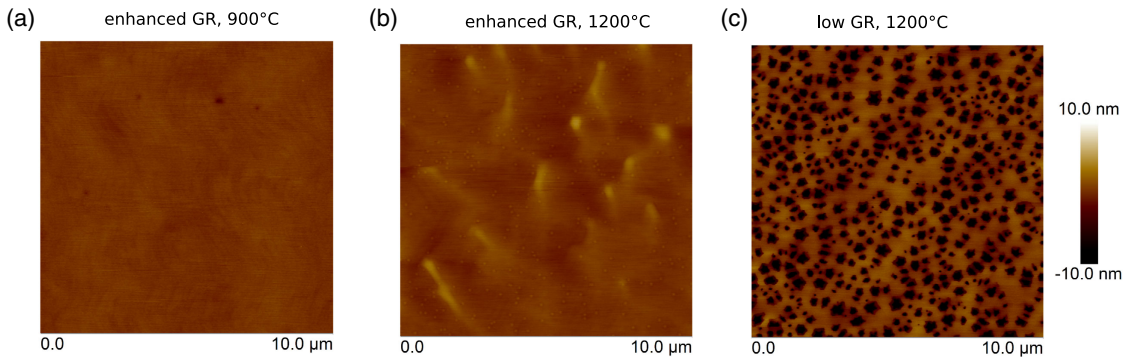

Figure 1. Atomic force microscopy (AFM) $10 \times 10\ \mu m^2$ scans showing the surface morphology of AlScN high-electron-mobility transistor (HEMT) structures grown on SiC with an enhanced growth rate (GR) at: a) 900 °C and b) 1200 °C and c) low GR at 1200 °C barrier growth temperature. Root mean square (RMS) values are: a) 0.31 nm and b) 0.58 nm and c) 4.56 nm.

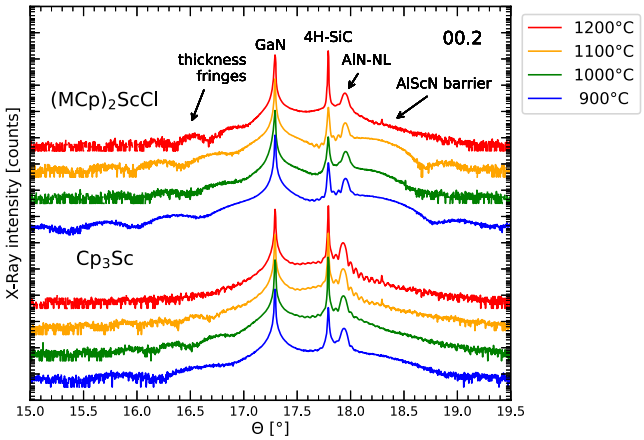

Figure 2. High-resolution X-Ray diffractometry (HRXRD) Θ/2Θ scans of the 00.2 reflections of the AlScN HEMT structures grown at 900, 1000, 1100, and 1200 °C with the Sc precursors $(MCp)_2ScCl$ and Cp_3Sc.

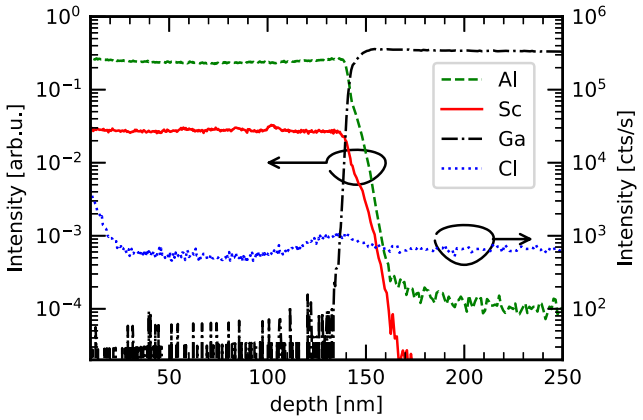

Figure 3. Secondary-ion mass spectrometry (SIMS) depth profile of a 150 nm thick $Al_{0.9}Sc_{0.1}N$ layer grown with $(MCp)_2ScCl$ as Sc precursor on an n-GaN buffer. The Al, Sc, and Ga signals were obtained as $AlCs^+$, $ScCs^+$, and $GaCs^+$ ions in the positive-ion detection mode (left *y*-axis). These signals were normalized to Cs_2^+ signal. The Cl signal was measured in the negative-ion mode (right *y*-axis).

(AlN-NL), the weaker and broader reflections of the thin AlScN barrier layers, which include diffusion-induced AlGaN interlayers, are visible. The AlScN peaks are more pronounced in the diffractograms of the $(MCp)_2ScCl$ samples. Since the total approximated thickness of barrier and diffusion-induced interlayers is the same for the samples grown with the different precursors, we assume that the AlScN barrier is thicker and the diffusion-induced AlGaN interlayer thinner in the samples grown with $(MCp)_2ScCl$, resulting in a more pronounced AlScN peaks in the diffractogram, while the AlScN barrier is thinner and the diffusion-induced AlGaN interlayer thicker in the samples grown with Cp_3Sc, resulting in broadened reflections. With increasing Sc content, the position of the AlScN peaks shifts toward lower angles and can be overlaid by the 4H-SiC and AlN nucleation layer peaks. We assume that this is the case for the samples grown at 1200 °C, as the Sc content increases with the growth temperature.[17] Thickness fringes of the thin AlScN barriers can be seen in the diffractograms as well. The absence of thickness fringes in the diffractogram of the sample grown with Cp_3Sc at 1200 °C indicates that the barrier/buffer interface was heavily degraded by interface diffusion. Considering these results, we conclude that the barrier/channel interface of the samples grown with the novel precursor is defined better than the one with the standard precursor. We assume that the halved growth time lowered the thermal budget significantly and reduced diffusion effects.

2.3. Compositional Characterization

Impurities in the Sc source were proven to have a strong negative effect on the chemical and electronic properties of AlScN/GaN heterostructures grown by MOCVD[17] and MBE[27]. In MOCVD growth, impurities can be introduced not only by a poorly purified source material but also by the precursor molecule itself. The standard precursor molecule Cp_3Sc contains 15 carbon atoms for each Sc atom, which means that a large amount of carbon is present in the gas phase during the MOCVD growth process. The novel precursor molecule $(MCp)_2ScCl$ contains only 12 carbon atoms for each Sc atom, which represents a notable reduction of carbon atoms introduced by the precursor molecule. The introduction of Cl into the precursor molecule was not found to have a negative effect on the grown layers. A secondary-ion mass spectrometry (SIMS) measurement of a 150 nm-thick $Al_{0.9}Sc_{0.1}N$ layer grown with $(MCp)_2ScCl$ as Sc precursor on an n-GaN buffer is shown in **Figure 3**. The Cl signal is close to the background level of our instrument and remains constant across the epilayer stack indicating that the chlorine content is below the detection limit in both the AlScN and the buffer layer.

2.4. Electrical Properties

The electrical properties of AlScN/GaN heterostructures are very sensitive to the quality of the Sc precursor. High impurity concentrations in the precursor, such as oxygen or metal traces, lead to high R_{sh}, low n_s and low μ in HEMT structures grown by MOCVD, especially at low growth temperatures of 900 and 1000 °C,[17] as well as to the degradation of the electrical properties of AlScN/n-GaN heterostructures grown by MBE.[27] Furthermore, the interface abruptness affects the electrical performance. This is directly related to the growth temperature. At a high temperature, the thermal budget for diffusion at the interfaces is high and leads to thick-graded AlGaN interlayers and an increase in R_{sh}.[18] Very low GR requires long growth times at high temperatures, increasing diffusion effects further. With $(MCp)_2ScCl$ as Sc precursor, we obtain R_{sh} that are by 20% lower than the ones achieved with Cp_3Sc in the temperature range of 900 to 1200 °C, as shown in **Figure 4**. All samples were grown without a nominal AlN interlayer. The lowest reported R_{sh} for MOCVD-grown AlScN HEMT structures is achieved at a barrier growth temperature of 900 °C. The sample has an Sc content of ≈10% and a barrier thickness of 7.2 nm, which includes the diffusion-induced AlGaN grading at the interface. The average R_{sh} is as low as 172 Ω sq^{-1} and homogeneous across the 4 in. wafer with a standard deviation of 1%. The average n_s is

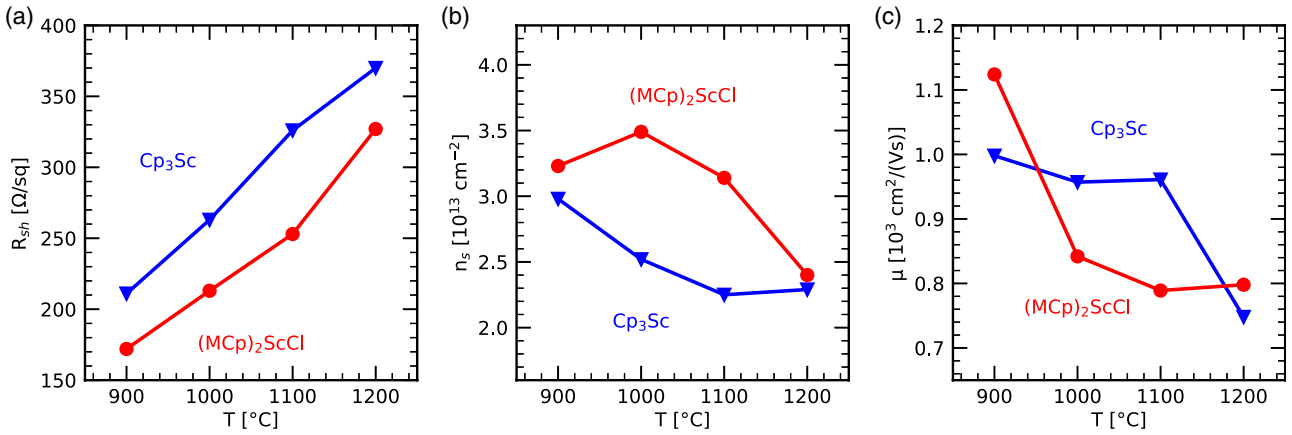

Figure 4. Contactless Hall measurements on AlScN HEMT structures grown on 4 H-SiC wafers with $(MCp)_2ScCl$ (red circles) at different temperatures. The values achieved with Cp_3Sc (blue triangles)[21] are shown for comparison. a) Sheet resistance R_{sh}, b) sheet charge carrier density n_s, and c) electron mobility μ are average values obtained for the 100 mm wafers. The solid lines are a guide to the eye.

3.2×10^{13}cm^{-2} and the average μ is 1124 cm^2 Vs^{-1}, both are homogeneous across the 4 in. wafer with a standard deviation of 2% and 3%, respectively. The fact that superior electrical performance was achieved at this low growth temperature indicates an improvement in the interface of barrier and channel, and that the new precursor´s impurity level is very low. To test the reproducibility, the 900 °C-sample was grown four times in total. The sheet resistance average value on the wafers varied ±3% which emphasizes the stability of the injection system and the reproducibility of the process. With increasing growth temperature, the R_{sh} increases to 327 Ω sq^{-1} at 1200 °C, while the n_s drops to 2.4×10^{13} cm^{-2} and the μ to 798 cm^2 Vs^{-1}. This indicates that the effect of the thermal budget cannot yet be counterbalanced by the GR increase. However, we have not only improved the results obtained with MOCVD, but to some extent also surpassed those grown by MBE reported in literature. In **Figure 5**, we show μ as a function of n_s of different AlScN HEMTs structures. A passivated MBE-grown structure with very high n_s of 6.2×10^{13} cm^{-2} and low μ of 340 cm^2 Vs^{-1} was demonstrated,[11] as well as an unpassivated structure with very high μ of 1556 cm^2 Vs^{-1} and moderate n_s of 2.4×10^{13} cm^{-2}.[27] The sheet resistances were 294 and 167 Ω sq^{-1}, respectively. With $(MCp)_2ScCl$ as Sc precurser, we managed to achieve a very low sheet resistance of 172Ω sq^{-1} at both high n_s and μ.

The novel precursor bis-methylcyclopentadienyl-scandium chloride ($(MCp)_2ScCl$) was used to grow AlScN HEMT structures. Thanks to its increased vapor pressure, it allows for doubling the AlScN GR. This results in a decreased thermal budget and therefore reduces interface diffusion. The electrical characteristics we report are among the best reported in the literature so far with at the same time high sheet charge carrier density n_s and electron mobility μ.

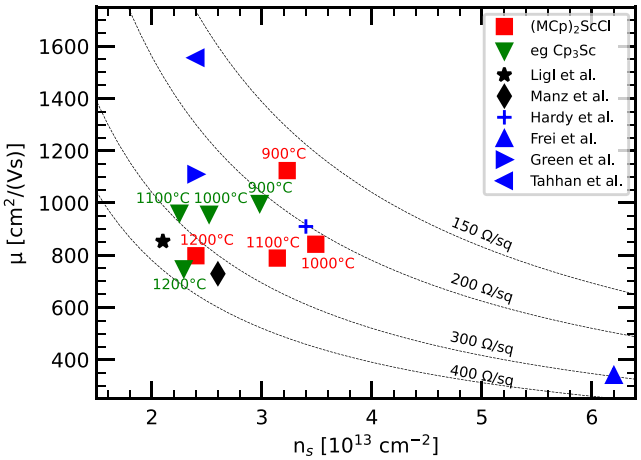

Figure 5. The electrical performance of AlScN HEMT structures grown with the novel precursor $(MCp)_2ScCl$ (red squares) is compared to the results obtained with Cp_3Sc (green triangles),[21] and our previously published results (black symbols),[17,18] as well as to the performance of AlScN HEMT structures grown by molecular beam epitaxy (MBE, blue symbols).[9,11,28,30] Lines of constant sheet resistance are indicated.

3. Experimental Section

The growth experiments were performed in a close-coupled showerhead MOCVD reactor capable of generating an adequate molar flow of the low-vapor pressure scandium precursor by a proprietary setup.[16] 4 in. *c*-plane Al_2O_3 and semi-insulating 4H-SiC substrates were used. The carrier gas was hydrogen while ammonia (NH_3) was used as the N source, trimethylgallium (TMGa) and trimethylaluminum (TMAl) as the group 13- or IIIA-precursors, and silane (SiH_4) as source gas for the in situ grown SiN_x cap layer. Two different electronic grade Sc precursors provided by Dockweiler Chemicals GmbH[24] were used: Cp_3Sc and $(MCp)_2ScCl$. The epilayer HEMT stack was the same as the ones described in our previous works.[17,18] It consists of an AlN nucleation layer and a GaN buffer designed to compensate background donor concentrations, made of a lower, Fe-doped GaN and an upper, non-intentionally doped GaN which serves also as a channel layer.[29] The ≈10 nm thick AlScN with an Sc content of ≈10% is grown directly on top and capped with a 5 nm thick SiN_x cap. With the use of $(MCp)_2ScCl$, we access higher GRs and half the barrier growth time from 20 min to 10 min by doubling TMAl flow. With each precursor, a barrier temperature series (900, 1000, 1100, 1200 °C) was grown on 4H-SiC substrates to examine the effect on the electrical performance and morphology. The V/III ratio was kept constant by using a NH_3 molar flow of 4.9×10^{-2} mol min^{-1}. Thick AlScN layers were grown on n-GaN buffers grown on sapphire substrates for structural characterization.

AFM in tapping mode was used to characterize the surface morphology by determining the RMS average. HRXRD Θ/2Θ -scans of the 00.2, 00.4, and 00.6 reflections combined with X-Ray reflectometry (XRR) measurements were employed to approximate the thicknesses of the barrier including diffusion-induced interlayers and the cap, respectively. The chemical composition of the layers was studied by SIMS utilizing a quadrupole system. The depth profiles were obtained by the bombardment at the incidence angle of 45° with respect to the surface normal using a primary beam of 1 keV Cs^+ ions. The uncertainty of the determined Sc content is ±2%. The impurities of oxygen, carbon, and chlorine incorporated in the layers could not be quantified due to the lack of standards but were examined qualitatively. The electrical properties of the HEMT structures were determined by eddy-current sheet resistance measurements and contactless Hall measurements using a Semilab mobility mapper.

Acknowledgements

This work was funded by the BMBF Project ProMat_KMU "PuSH" Grant Number 03XP0387B. The authors thank Nadine Brückner (Fraunhofer IAF) for HRXRD measurements and Hanspeter Menner (Fraunhofer IAF) for his support on the hardware. Furthermore, Dockweiler Chemicals GmbH is gratefully acknowledged for having supplied the Sc precursors for this study and fruitful discussions.

Open Access funding enabled and organized by Projekt DEAL.

Conflict of Interest

The authors declare no conflict of interest.

Data Availability Statement

The data that support the findings of this study are available from the corresponding author upon reasonable request.

Keywords

AlScN, high-electron-mobility transistors, metal–organic chemical vapor deposition, ScAlN, vapor pressure

Received: October 7, 2022
Revised: October 20, 2022
Published online:

[1] R. Quay, P. Brückner, A. Tessmann, E. Ture, D. Schwantuschke, M. Dammann, P. Waltereit, in *Integrated Nonlinear Microwave and Millimetre-wave Circuits Workshop (INMMiC)*, IEEE, Graz, Austria **2017**, pp. 1–3.
[2] X. Ding, Y. Zhou, J. Cheng, *CES Trans. Electr. Mach. Syst.* **2019**, *3*, 54.
[3] M. Meneghini, C. de Santi, I. Abid, M. Buffolo, M. Cioni, R. A. Khadar, L. Nela, N. Zagni, A. Chini, F. Medjdoub, G. Meneghesso, G. Verzellesi, E. Zanoni, E. Matioli, *J. Appl. Phys.* **2021**, *130*, 181101.
[4] M. Hardy, D. Meyer, N. Nepal, B. Downey, D. Scott Katzer, D. Storm, in *IEEE MTT-S International Microwave Workshop Series on Advanced Materials and Processes for RF and THz Applications (IMWS-AMP)*, IEEE, Piscataway, NJ pp. 1–3.
[5] T. E. Kazior, E. M. Chumbes, B. Schultz, J. Logan, D. J. Meyer, M. T. Hardy, in *IEEE MTT-S International Microwave Symposium (IMS)*, IEEE, Piscataway, NJ **2019** pp. 1136–1139.
[6] O. Ambacher, B. Christian, M. Yassine, M. Baeumler, S. Leone, R. Quay, *J. Appl. Phys.* **2021**, *129*, 204501.
[7] S. Zhang, W. Y. Fu, D. Holec, C. J. Humphreys, M. A. Moram, *J. Appl. Phys.* **2013**, *114*, 243516.
[8] D. F. Storm, D. A. Deen, D. S. Katzer, D. J. Meyer, S. C. Binari, T. Gougousi, T. Paskova, E. A. Preble, K. R. Evans, D. J. Smith, *J. Cryst. Growth* **2013**, *380*, 14.
[9] M. T. Hardy, B. P. Downey, N. Nepal, D. F. Storm, D. S. Katzer, D. J. Meyer, *Appl. Phys. Lett.* **2017**, *110*, 162104.
[10] M. T. Hardy, B. P. Downey, N. Nepal, D. F. Storm, D. S. Katzer, D. J. Meyer, *ECS Trans.* **2017**, *80*, 161.
[11] K. Frei, R. Trejo-Hernández, S. Schütt, L. Kirste, M. Prescher, R. Aidam, S. Müller, P. Waltereit, O. Ambacher, M. Fiederle, *Jpn. J. Appl. Phys.* **2019**, *58*, SC SC1045.
[12] J. Casamento, C. S. Chang, Y.-T. Shao, J. Wright, D. A. Muller, H. Xing, D. Jena, *Appl. Phys. Lett.* **2020**, *117*, 112101.
[13] P. Wang, D. A. Laleyan, A. Pandey, Y. Sun, Z. Mi, *Appl. Phys. Lett.* **2020**, *116*, 151903.
[14] D. Koleske, J. Knapp, S. Lee, M. Crawford, J. Creighton, K. Cross, G. Thaler, Issues Associated with the Metalorganic Chemical Vapor Deposition of ScGaN and YGaN Alloys, Sandia National Laboratories, Albuquerque, New Mexico **2009**.
[15] C. Saidi, N. Chaaben, A. Bchetnia, A. Fouzri, N. Sakly, B. El Jani, *Superlattices Microstruct.* **2013**, *60*, 120.
[16] S. Leone, J. Ligl, C. Manz, L. Kirste, T. Fuchs, H. Menner, M. Prescher, J. Wiegert, A. Žukauskaite, R. Quay, O. Ambacher, *Phys. Status Solidi RRL* **2020**, *14*, 1900535.
[17] J. Ligl, S. Leone, C. Manz, L. Kirste, P. Doering, T. Fuchs, M. Prescher, O. Ambacher, *J. Appl. Phys.* **2020**, *127*, 195704.
[18] C. Manz, S. Leone, L. Kirste, J. Ligl, K. Frei, T. Fuchs, M. Prescher, P. Waltereit, M. A. Verheijen, A. Graff, M. Simon-Najasek, F. Altmann, M. Fiederle, O. Ambacher, *Semicond. Sci. Technol.* **2021**, *36*, 034003.
[19] B.-J. Godejohann, E. Ture, S. Müller, M. Prescher, L. Kirste, R. Aidam, V. Polyakov, P. Brückner, S. Breuer, K. Köhler, R. Quay, O. Ambacher, *Phys. Status Solidi B* **2017**, *254*, 1600715.
[20] H. Yu, B. Parvais, M. Zhao, R. Rodriguez, U. Peralagu, A. Alian, N. Collaert, *Appl. Phys. Lett.* **2022**, *120*, 213504.
[21] I. Streicher, S. Leone, C. Manz, L. Kirste, M. Prescher, P. Waltereit, M. Mikulla, R. Quay, O. Ambacher, *Cryst. Growth Des.* **2022**, Unpublished.
[22] S. Fichtner, N. Wolff, F. Lofink, L. Kienle, B. Wagner, *J. Appl. Phys.* **2019**, *125*, 114103.
[23] P. Wang, D. Wang, N. M. Vu, T. Chiang, J. T. Heron, Z. Mi, *Appl. Phys. Lett.* **2021**, *118*, 223504.
[24] Dockweiler Chemicals, https://dockchemicals.com/.
[25] S. Leone, C. Manz, H. Menner, J. Wiegert, J. Ligl, Verfahren und Vorrichtung zur Herstellung einer Schicht und Damit Versehenes Substrat: Patent Application Publication, *EP 3786321*, **2021**.
[26] S. Leone, C. Manz, H. Menner, J. Wiegert, J. Ligl, Method and Apparatus for Manufacturing a Semiconductor Layer and Substrate Provided Therewidth: Patent Application Publication, *US 2021/0066070 A1*, **2021**.
[27] J. Casamento, H. Lee, C. S. Chang, M. F. Besser, T. Maeda, D. A. Muller, H. Xing, D. Jena, *APL Mater.* **2021**, *9*, 091106.
[28] M. B. Tahhan, J. A. Logan, M. T. Hardy, M. G. Ancona, B. Schultz, B. Appleton, T. Kazior, D. J. Meyer, E. M. Chumbes, *IEEE Trans. Electron Devices* **2022**, *69*, 962.
[29] S. Leone, F. Benkhelifa, L. Kirste, C. Manz, S. Mueller, R. Quay, T. Stadelmann, *Phys. Status Solidi B* **2018**, *255*, 1700377.
[30] A. J. Green, N. Moser, N. C. Miller, K. J. Liddy, M. Lindquist, M. Elliot, J. K. Gillespie, R. C. Fitch, R. Gilbert, D. E. Walker, E. Werner, A. Crespo, E. Beam, A. Xie, C. Lee, Y. Cao, K. D. Chabak, *IEEE Electron Device Lett.* **2020**, *41*, 1181.